

# Clustering segregation of Lyman Alpha Emitter Galaxies at z=2.1

Harold Francke<sup>1\*</sup>, Eric Gawiser<sup>2</sup>, Lucia Guaita<sup>3</sup>, Ana Matkovic<sup>4</sup>, Robin Ciardullo<sup>4</sup>, Caryl Gronwall<sup>4</sup>, Leopoldo Infante<sup>1</sup>, Nelson Padilla<sup>1</sup> and the MUSYC Collaboration

<sup>1</sup> Pontificia Universidad Católica de Chile, <sup>2</sup> Rutgers University, <sup>3</sup> Stockholm University, <sup>4</sup> Penn State University; \* email: hfrancke@astro.puc.cl

## Abstract:

We present updated results on large scale structure clustering strength of z=2.1 Lyman Alpha Emitters (LAE) in the MUSYC survey. This survey comprises 4 fields of 30x30 arcmin each, which have been imaged both in broadband UBVRIZ (Gawiser et al. 2006) and narrow-band OII 3727 filters, allowing for the selection of LAEs at this redshift (Guaita et al. 2010). Here we present the joint clustering analysis for two of the four fields: E-CDFS and SDSS1030+05. With the additional sample, we were able to measure the dependence of correlation length  $r_0$  with Lyman-Alpha line luminosity and equivalent width (EW), as estimated from the narrow- and broadband photometry. We observe significant correlations of clustering strength with both quantities.

## Observations and sample selection

We used OII (NB3727, green), U (purple) and B (blue) photometry to select LAEs as in Guaita et al. (2010) (see fig. 1 on the right). The narrow-band imaging was obtained in two runs on CTIO Blanco 4m+Mosaic II, with a 5 $\sigma$  detection limiting magnitude of NB3727=25.1 (AB) on both fields, and same reductions and procedure for the new SDSS1030+05 data. Due to the non-square shape of the NB3727 filter (see inset of fig. 1), fainter and/or low EW sources are not detected in the borders of the filter. This affects the widths of the redshift distributions of faint versus bright sources and thus clustering measurements. We take into account these effects by performing a Monte-Carlo simulation of the LAE selection process, having luminosity and EW distributions following Gronwall et al. (2007), including photometric errors and the same selection applied to the data.

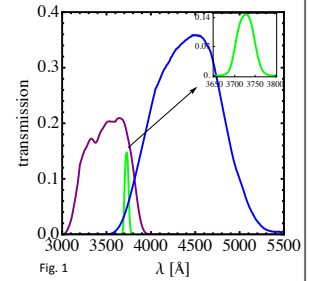


Fig. 1

To statistically estimate Ly $\alpha$  luminosity and EW from photometry alone, we used the same approach as Guaita et al. (2010), subtracting the continuum flux contribution from the line flux and using an average estimation of the narrow-band filter transmission. The same estimation was used in the simulations to assess the effect of photometric errors and filter shape in these estimations.

Fig. 2 (left) shows the Ly $\alpha$  luminosity and restframe EW distribution of sources in SDSS1030+05 (filled circles) and ECF-5 (open boxes) fields. Red solid line shows the 5 $\sigma$  detection limit of the survey, black solid line shows the 20 $\text{\AA}$  EW cut, dotted gray lines show the separation between samples, and black dashed lines have constant continuum luminosity of  $\log(L_c) = (-29.4, -29.8, -30.2)$ . Notice that the faint sample ( $\log(L) < 42.1$ ) is not complete in EW distribution, and that both low and high EW samples do not include these faint sources.

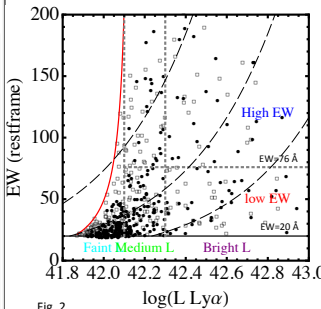


Fig. 2

## Luminosity Segregation

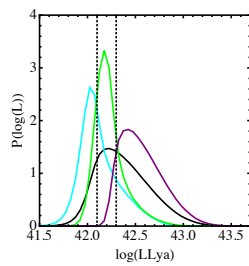


Fig. 3: Expected true luminosity distributions of the whole (black), low (cyan), medium (green) and high estimated luminosity (purple) samples of LAEs, determined from the monte-carlo simulation. The vertical dotted line marks the separation between samples, at  $\log(L) = (<42.1, 42.1 < L < 42.3$  and  $>42.3$ ). Fainter samples have a long tail to higher luminosities due to the sources that have their fluxes underestimated in the border of the OII filter.

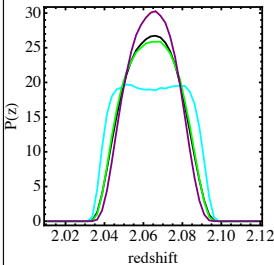


Fig. 4: Redshift distributions of the selected samples of LAEs (same colors), also from the simulation. The black and green distributions are nearly identical, while the FWHM of the purple and cyan curves is 10% smaller and 22% bigger than the black one, respectively.

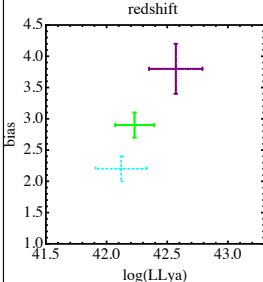


Fig. 5: Clustering strength, given by the linear bias factor as a function of Ly $\alpha$  luminosity. The bias factor here is defined as  $\sigma_{8, \text{LAE}} / \sigma_{8, \text{DM}}$ . The bright end of our LAE sample seems to cluster significantly more than the faint end, although more data is required to robustly establish a trend. Ouchi et al. (2010) presents a similar comparison but with negative results at this redshift. Colors are same as above, but notice cyan point is not complete in EW space.

## Equivalent Width Segregation

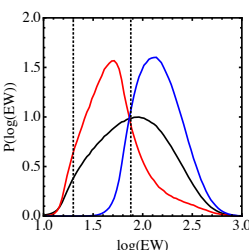


Fig. 6: Left: Expected restframe Ly $\alpha$  equivalent width (EW) distributions for the whole (black), low EW (red) and high EW (blue) samples. Dotted lines mark the EW cut and separation between samples, at  $\log(EW) = 1.3$  and  $1.88$ . Right: Redshift distribution of the two EW-separated samples. The blue distribution's FWHM is 24% smaller than the red one.

## Results

With our increased sample of LAEs, we present updated results for the clustering of LAEs at z=2.1 in MUSYC (see table below). We confirmed the result from Guaita et al. (2010) for the full sample, namely that the bulk population of these galaxies could be the progenitors of a significant fraction of L\* galaxies in the present Universe. We also found preliminary indications that these LAEs show a significant trend of increasing  $r_0$  with line luminosity, and decreasing with equivalent width. This is somewhat at odds with models that predict only a mild dependence with luminosity (e.g. Orsi et al. 2008). Since for star-forming galaxies it has been previously shown that clustering strength scales with continuum luminosity, our results could be a reflection of this effect on Ly $\alpha$  luminosity and EW at the low end of the luminosity function. Because these these quantities are correlated, however, more work is needed in order to disentangle the real trend from selection effects, and more data to confirm and constrain these trends accurately.

Sample	n <sup>o</sup> of LAEs	bias
Whole	540	1.8 +/- 0.1
Faint L	243	2.2 +/- 0.2
Medium L	194	2.9 +/- 0.2
Bright L	103	3.8 +/- 0.4
low EW	184	3.9 +/- 0.3
high EW	113	2.9 +/- 0.4

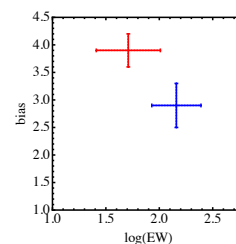


Fig. 7: Clustering results for the low-EW and high-EW samples. There is some evidence of a trend of decreasing clustering strength with EW.